

# Buckling Behaviour of Laminated Composite Plates Under Thermal Loading

P.S. Simelane and B. Sun

*Centre for Research in Applied Technology and Department of Mechanical Engineering  
Peninsula Technikon, P.O. Box 1906, Bellville, 7535, Cape Town, South Africa  
[Sunb@mail.pentech.ac.za](mailto:Sunb@mail.pentech.ac.za)*

## ABSTRACT

A thermal buckling analysis of composite laminated plate is studied using the ABAQUS/Standard Finite Element simulation package. The effects of transverse shear deformation are accounted for by the use of the Mindlin first-order shear deformation (FSDT) theory on a plate of rectangular construction. The plate has antisymmetric lamination with respect to the middle plane. The intermediate class of deformation is employed for this non-linear analysis. The first variation of the total potential energy establishes the equilibrium equation and the second variation analyses the stability of the laminated composite. A displacement-based finite element with five degrees of freedom in each node is used. The effects of lamination angle, modulus ratio, plate aspect ratio, plate thickness ratio and boundary constraints upon the critical buckling temperature are investigated and found to have a significant effect on the critical buckling temperature, especially the number of layers.

## INTRODUCTION

Fiber-reinforced composites have found wider applications in recent years and this has resulted in renewed interest in their study under elevated temperatures. Studies have been conducted of the laminated composites under inplane mechanical loading and to a certain extent thermal loading has been investigated, but thermal buckling remains one of the

challenges facing the aerospace and other industries. Shaikh *et al.* /1/ proposed a higher-order theory of laminated composite plates and shells under thermal and static loading. Zeggane and Sridharan /2/ used the Reissner-Mindlin 'infinite strip' to study the stability of long laminated composite plates. Chandrashekhara /3/ investigated thermal buckling of laminated plates using a shear flexible finite element. Chen *et al.* /4/ used the eight-noded Serendipity finite element to study thermal buckling under uniform and nonuniform temperature distribution. Mathew *et al.* /5/ analysed an antisymmetric cross-ply composite laminate using a one-dimensional finite element having two nodes and six-degrees of freedom.

This paper incorporates transverse shear stiffness as part of the finite element analysis. This is because bending-extension coupling in this type of structure requires that the effect of transverse shear deformation be not ignored, as is usually done by the classical laminated plate theory /3/. The importance of accounting for shear deformation cannot be underestimated given the high ratio of inplane modulus to transverse shear modulus, especially under thermal loading conditions. Perhaps under different loading conditions the coupling would be not as effective, but subjecting a laminated composite plate to a change in temperature means that not only does the matrix-fiber arrangement experience the coupling phenomenon because of the difference materials that constitute the lamina, but the interface between the laminae that make up the stack would have to be considered, seeing that

each lamina would tend to expand or contract differently according to the stacking sequence. This is because there are two Poisson ratios: one giving the transverse strain caused by an axially applied stress and the other gives the axial strain caused by a transversely applied stress. The two are not independent but are related /9/.

In /14/ an approximation to thin shell theory is used for the buckling of cylindrical laminated composite panel with a circular hole. These shell elements are not "universally applicable to the analysis of composites since transverse shear effects can be significant in such cases" /14/. However, a relatively large number of laminae and the symmetrical lay-up will tend to minimise the importance of transverse shear deformation. The results in this paper will also show this to be the case, in that as the number of layers increases, the values of the critical buckling temperature tend not to deviate considerably from each of the stacking sequences.

In general, if the operating or service temperature is different from the curing temperature during the fabrication process, thermal stresses will arise. In this particular study the assumptions are that the laminate thickness is small compared to its lateral dimensions. This means that the stresses acting on the interlaminar planes in the interior of the laminate, that is, away from the free edges, are negligibly small. Also there exists a perfect bond between any two laminae, and this implies that the laminae cannot slide over each other and the displacements across the bond are continuous. There exists also a perfect bond between the matrix and the fibrous material. Finally there are no empty spaces in the whole laminated composite. The present work uses the stiffnesses in the appropriate directions as will be indicated in the Results and Discussion section.

## PROBLEM STATEMENT

As in metallic structures, changes in temperatures are commonplace in composite structures during fabrication and structural usage. Changes in temperature result in expansion when the material is heated, and contraction when cooled, and in most cases this

expansion is proportional to the temperature change. The equation governing the behaviour of a laminated composite under thermal loading is given by

$$\begin{pmatrix} \{N\} \\ \{M\} \\ \{Q\} \end{pmatrix} = \begin{pmatrix} [A] & [B] & 0 \\ [B] & [D] & 0 \\ 0 & 0 & [A] \end{pmatrix} \begin{pmatrix} \{\epsilon\} \\ \{\kappa\} \\ \{\gamma\} \end{pmatrix} - \begin{pmatrix} [N_t] \\ [M_t] \\ 0 \end{pmatrix} \quad (1)$$

where extensional stiffness  $A_{ij}$ , flexural-extensional coupling stiffness  $B_{ij}$ , and flexural stiffness  $D_{ij}$  of the plate are defined as

$$(A_{ij}, B_{ij}, D_{ij}) = \sum_{k=1}^N \int_{z_{k-1}}^{z_k} (\bar{Q}_{ij})_k (1, z, z^2) dz \quad (i, j = 1, 2, 6)$$

$$(\bar{A}_{ij}) = \beta \sum_{k=1}^N \int_{z_{k-1}}^{z_k} (\bar{Q}_{ij})_k dz \quad (i, j = 4, 5)$$

$\beta$  is the shear correction factor /7/.

## MATHEMATICAL MODEL

Based on the Mindlin plate theory /6/, the deformation field can be written in the following form

$$\begin{aligned} u(x, y, z) &= u_0(x, y) + z\theta_x(x, y) \\ v(x, y, z) &= v_0(x, y) + z\theta_y(x, y) \\ w(x, y, z) &= w_0(x, y) \end{aligned} \quad (2)$$

where  $u_0$ ,  $v_0$  and  $w_0$  are the displacements of the reference surface in the  $x$ ,  $y$  and  $z$  direction, respectively, and  $\theta_x$ ,  $\theta_y$  are the rotations of the transverse normal about the  $x$ - and  $y$ -axes. The intermediate class of deformation is defined by the limitations that the strains be small compared with unity, the rotations relative to the  $x$  and  $y$  directions moderately small, and that the  $\bar{\epsilon}_x$ ,  $\bar{\epsilon}_y$ ,  $\bar{\gamma}_{xy}$ ,  $\bar{\gamma}_{yz}$  and  $\bar{\gamma}_{xz}$  components of the strain-displacement relations for a three-dimensional medium, including thermal strains are

$$\begin{aligned} \{\epsilon\} &= (\bar{\epsilon}_x \quad \bar{\epsilon}_y \quad \bar{\gamma}_{xy})^T + \\ &\quad \zeta (\bar{\kappa}_x \quad \bar{\kappa}_y \quad \bar{\kappa}_{xy})^T - (\alpha_x \quad \alpha_y \quad \alpha_{xy})^T \Delta T \end{aligned}$$

$$\{\gamma\} = \begin{pmatrix} \bar{\gamma}_{yz} & \bar{\gamma}_{xz} \end{pmatrix}^T = \begin{pmatrix} w_{,y} + \theta_y & w_{,x} + \theta_x \end{pmatrix}^T \quad (3)$$

where

$$\begin{pmatrix} \bar{\epsilon}_x & \bar{\epsilon}_y & \bar{\gamma}_{xy} \end{pmatrix}^T = \begin{pmatrix} u_{,x} & v_{,y} & u_{,y} + v_{,x} \end{pmatrix}^T + \frac{1}{2} \begin{pmatrix} \varphi_x^2 & \varphi_y^2 & 2\varphi_x\varphi_y \end{pmatrix}^T$$

$$\begin{pmatrix} \bar{\kappa}_x & \bar{\kappa}_y & \bar{\kappa}_{xy} \end{pmatrix} = \begin{pmatrix} \theta_{x,x} & \theta_{y,y} & \theta_{x,y} + \theta_{y,x} \end{pmatrix} \quad (4)$$

$\bar{\epsilon}_x, \bar{\epsilon}_y, \bar{\gamma}_{xy}, \bar{\gamma}_{yz}$  and  $\bar{\gamma}_{xz}$  are extensional and shearing strains at any point through the plate thickness and  $\epsilon_x, \epsilon_y$  and  $\gamma_{xy}$  denote the corresponding quantities at points on the plate middle plane only. We note that

$$\varphi_x = w_{,x} \quad \varphi_y = w_{,y}$$

where “ $_x$ ” and “ $_y$ ” represent partial differentiation with respect to  $x$  and  $y$ . The stress-strain relation of the  $k$ -th layer of a laminated composite plate is given by

$$\begin{pmatrix} \sigma_x \\ \sigma_y \\ \tau_{xy} \end{pmatrix} = \begin{bmatrix} \bar{Q}_{11} & \bar{Q}_{12} & \bar{Q}_{16} \\ \bar{Q}_{12} & \bar{Q}_{22} & \bar{Q}_{26} \\ \bar{Q}_{16} & \bar{Q}_{26} & \bar{Q}_{66} \end{bmatrix} \left( \begin{pmatrix} \epsilon_x \\ \epsilon_y \\ \gamma_{xy} \end{pmatrix} + z \begin{pmatrix} \theta_{x,x} \\ \theta_{y,y} \\ \theta_{x,y} + \theta_{y,x} \end{pmatrix} \right) - \begin{bmatrix} \bar{Q}_{11} & \bar{Q}_{12} & \bar{Q}_{13} \\ \bar{Q}_{12} & \bar{Q}_{22} & \bar{Q}_{23} \\ \bar{Q}_{13} & \bar{Q}_{23} & \bar{Q}_{33} \end{bmatrix} \begin{pmatrix} \alpha_x \\ \alpha_y \\ 2\alpha_{xy} \end{pmatrix} \Delta T$$

$$\begin{pmatrix} \tau_{xz} \\ \tau_{yz} \end{pmatrix} = \begin{pmatrix} \bar{Q}_{44} & \bar{Q}_{45} \\ \bar{Q}_{45} & \bar{Q}_{55} \end{pmatrix} \begin{pmatrix} \gamma_{xz} \\ \gamma_{yz} \end{pmatrix} \quad (5)$$

where  $\alpha_i$  are thermal expansion coefficients in the principal material directions.  $\Delta T$  is the temperature rise. In the derivation of the above equations, the stresses and strains were transformed from the principal material directions of the orthotropic lamina to the  $x, y$  coordinate system according to

$$T_{ij} = a_{ik} a_{jl} T_{kl} \quad (6)$$

From the general plate theory we know that

$$\{N\}^T = (N_x, N_y, N_{xy}) = \int_{-\frac{h}{2}}^{\frac{h}{2}} (\sigma_x, \sigma_y, \tau_{xy}) dz$$

$$\{M\}^T = (M_x, M_y, M_{xy}) = \int_{-\frac{h}{2}}^{\frac{h}{2}} (\sigma_x, \sigma_y, \tau_{xy}) z dz$$

$$\{Q\}^T = (Q_x, Q_y) = \int_{-\frac{h}{2}}^{\frac{h}{2}} (\tau_{xz}, \tau_{yz}) dz \quad (7)$$

where  $N$ ,  $M$ , and  $Q$  are the inplane, bending and shear stress resultants over the thickness of the plate. The use of Mindlin plate theory together with the intermediate class of deformation and the general plate theory results in the stress-strain relation of the form of equation (1). The stress state developed in the plate very much depends on the lay-up and boundary conditions, and it is this stress state that is responsible for plate buckling rather than the applied one. The loss of stability is analysed by setting  $u = u_0 + u_1$ ,  $v = v_0 + v_1$ ,  $w = w_0 + w_1$ ,  $\theta_x = \theta_{x0} + \theta_{x1}$ , and  $\theta_y = \theta_{y0} + \theta_{y1}$ , where the subscript “1” denotes the incremental displacement on the primary path of equation (1).

## FINITE ELEMENT MODEL

For a conservative structural system, the total potential energy  $\Pi$  of a loaded structure is defined as the sum of the strain energy of the structure itself and the potential energy of the applied load.

$$\Pi = \Pi_m + \Pi_b + \Pi_s \quad (8)$$

where  $m$ ,  $b$ , and  $s$  are the membrane, bending and shear strain energies, respectively. The problem is solved by dividing the region  $\Omega$  of the plate into  $n$ -noded quadrilateral finite elements, each with five degrees of freedom per node, such that

$$\Pi(\mathbf{a}) = \sum_{i=1}^n \Pi^e(\mathbf{a}) \quad (9)$$

where  $\Pi$  and  $\Pi^e$  are potential energies of the plate and element, respectively,  $\mathbf{a}$  is the displacement vector

$\{u_1, v_1, w_1, \theta_{x1}, \theta_{y1}\}$ . The variation in each element can be interpolated, for node  $i$  ( $i = 1, 2, \dots, n$ ), as

$$\begin{aligned} u_1 &= \sum_{i=1}^n N_i u_1^i \quad v_1 = \sum_{i=1}^n N_i v_1^i \quad w_1 = \sum_{i=1}^n N_i w_1^i \\ \theta_{x1} &= \sum_{i=1}^n N_i \theta_{x1}^i \quad \theta_{y1} = \sum_{i=1}^n N_i \theta_{y1}^i \end{aligned} \quad (10)$$

where  $N_i$  are the interpolation functions. Using the same shape function associated with node  $i$ , we can write

$$u_1 = \sum_{i=1}^4 N_i a_1^i \quad (11)$$

where  $N_i$  are the interpolation functions and are used to interpolate both the nodal in-plane displacements  $u$ ,  $v$ , the lateral displacement  $w$  as well as the normal rotation  $\theta_x$ ,  $\theta_y$ . The shape functions are expressed in terms of the natural (local) element co-ordinate system  $(\xi, \eta)$ .  $u_1$  is the element displacement vector and  $a_1^i$  is the vector of variables for node  $i$  in the element  $e$ . The normal and shear strain matrices and the curvature matrix are given by

$$\epsilon_{1t} = \sum_{i=1}^n B_{ti} a_1^i \quad \epsilon_{1b} = \sum_{i=1}^n B_{bi} a_1^i \quad \epsilon_{1s} = \sum_{i=1}^n B_{si} a_1^i \quad (12)$$

where  $B_{ti}$ ,  $B_{bi}$ , and  $B_{si}$  are, respectively, the normal-, shear- and curvature-displacement matrix associated with element  $e$ . The bending stresses and the shear stresses are defined as

$$\sigma = \sum_{i=1}^4 (A B_{ti} + B_d B_{bi}) a_1^i \quad \tau = \sum_{i=1}^4 \bar{A} B_{si} a_1^i \quad (13)$$

where,  $A$ ,  $B_d$  and  $\bar{A}$  material property matrices of the laminated composite as defined in equation (1). Using the constitutive equations, we have

$$\begin{aligned} \{N_1\} &= [A [B_{ti}] + [B_d [B_{bi}]]] \{a_1^i\} \\ \{M_1\} &= [B_d [B_{ti}] + [D [B_{bi}]]] \{a_1^i\} \end{aligned}$$

$$\{Q_1\} = [\bar{A}] [B_{si}] \{a_1^i\} \quad (14)$$

Substituting into the second variation of equation (9), and for arbitrary  $\delta u_1$ ,  $\delta v_1$ ,  $\delta w_1$ ,  $\delta \theta_1$ ,  $\delta \theta_1$  we have

$$\begin{aligned} &[K_1] \{a_1^i\} + [K_2] \{a_1^i\} + [K_3] \{a_1^i\} + \\ &[K_4] \{a_1^i\} + [K_5] \{a_1^i\} + [K_g] \{a_1^i\} = 0 \\ \text{and } &([K] + [K_g]) \{a_1^i\} = 0 \end{aligned} \quad (15)$$

where  $[K]$  is the structural stiffness matrix and  $[K_g]$  is the geometric stiffness matrix. Due to space limitations the full form of  $[K]$  and  $[K_g]$  cannot be given in this paper.

Classical eigenvalue buckling analysis is often used to estimate the critical (buckling) load of "stiff" structures such as the laminated composite. "Stiff" structures are those that carry design loads primarily by axial or membrane action, rather than by bending action. Their response usually involves very little deformation prior to buckling. In the finite element context, the classical eigenvalue-buckling problem may be stated as follows /8/. Given a structure with an elastic stiffness matrix,  $K_{ij}^{ij}$ , a loading pattern defined by the vector  $\{N_i\}$ , and an initial stress and loading stiffness matrix,  $K_g^{ij}$ , find load multipliers (eigenvalues),  $\lambda_i$ , and buckling mode shapes (eigenvectors),  $a_1^i$ , which satisfy equation (15). The critical buckling loads are then given by  $\lambda_i N^j$ . In this study only the smallest load multiplier and its associated mode shape are of interest. The eigenvector  $a_1^j$  associated with  $\lambda_{cr}$  defines the buckling mode.

## RESULTS AND DISCUSSION

The study is performed using a 4 x 4, 9-noded doubly curved thin shell element, with reduced integration and five degrees of freedom per node (S9R5). However, to account for the transverse shear deformation, the transverse shear of 5/6 is introduced in the ABAQUS/Standard input file.

## Isotropic Square Plate

In order to establish a benchmark or the integrity of the present analysis, the critical buckling temperatures of a simply supported square isotropic plate subjected to a uniform temperature increase are compared with those of Chandrashekhara /3/ in Table 1. The dimensions are  $a = b = 10\text{mm}$  and thickness  $t = 0.1\text{mm}$  with the following boundary conditions

Simply supported edges	Clamped edges
$x = 0, a \quad u_0 = w_0 = \theta_y = 0$	$x = 0, a \quad u_0 = v_0 = w_0 = \theta_x = \theta_y = 0$
$y = 0, b \quad v_0 = w_0 = \theta_x = 0$	$y = 0, b \quad u_0 = v_0 = w_0 = \theta_x = \theta_y = 0$

The following non-dimensional buckling temperatures were obtained in the ABAQUS/Standard computer simulations.

$$E = 1.0 \text{ GPa}, \nu = 0.3, a/t = 100,$$

$$a = b = 10, \alpha = 1.0 \times 10^{-6}/^\circ\text{C}$$

**Table 1**

Comparison of nondimensional critical buckling temperature for a simply supported isotropic thin plate

a/b	$\alpha T_{cr} \times 10^{-4}$	
	Present	Ref. /9/
0.25	0.6730	0.6727
0.50	0.7916	0.7913
0.75	0.9892	0.989
1.00	1.2659	1.2657
1.25	1.6214	1.6234
1.50	2.0558	2.0561
1.75	2.5691	2.5696
2.00	3.1607	3.1617

The results of the present analysis and reference /3/ are in excellent agreement. The next step is to change the properties of the isotropic plate to those of a laminated composite, and this is done throughout the remainder of this paper.

## Laminated Square Plate

The properties associated with the shell elements used in this composite analysis are:

- the thickness of the plate
- the number of integration points
- the material, in this case the lamina and
- the orientation of each layer

In the analysis of a laminated, orthotropic, composite plate, each layer has the same material properties. The effects of the various parameters are studied and the graphs are used to show the trends as these parameters are changed. Two sets of graphs are shown for each type of analysis, one for simply supported edges and another for clamped edges. Unless otherwise stated, each lamina has the following material properties;

**Table 2**

Material properties of a composite

$\nu_{12}$	$\alpha_{11}$	$\alpha_{12}$	$K_{11}$	$K_{22}$
0.28	0.02	22.5	2.987	2.587
$E_{11}$	$E_{22}$	$G_{12}$	$G_{13}$	$G_{23}$
181.0	10.30	7.17	7.17	6.21

where the 1-direction is along the fibres, the 2-direction is transverse to the fibres in the surface of the lamina, and the 3-direction is normal to the lamina, Figure 1 (a).  $E_{11}$ ,  $E_{22}$ ,  $G_{12}$ ,  $G_{13}$  and  $G_{23}$  are in  $10^9$  Pascals and  $\alpha_{11}$  and  $\alpha_{12}$  are in  $10^{-6}$  per degrees Celsius. Figure 1 (b) shows the dimensions and co-ordinates of a typically stacked laminate.

## Effect of ply orientation

Figure 2 shows the critical buckling temperature  $T_{cr}$  versus lamination angle  $\psi$  for a simply supported and clamped plate. The variation in lamination angle  $\psi$  may result in large changes of  $T_{cr}$  as shown by the figure. Also the critical buckling temperature for a given thickness of laminated plates increases as the number of layers,  $N$ , increases. The maximum value of  $T_{cr}$  occurs at  $\psi = 45^\circ$  for clamped  $N = 4$  and  $N = 8$  plates.

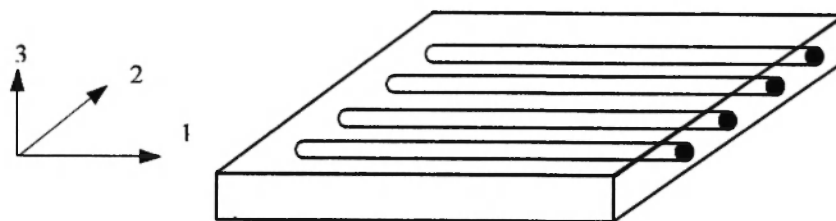


Fig. 1(a): A typical lamina

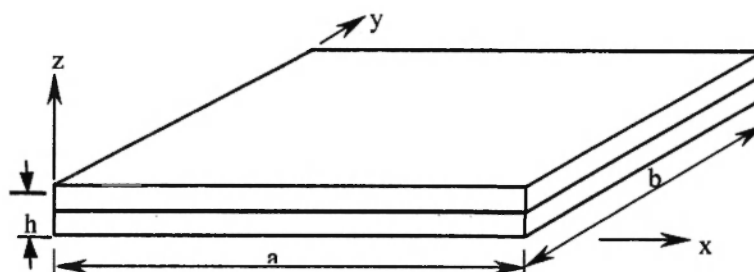
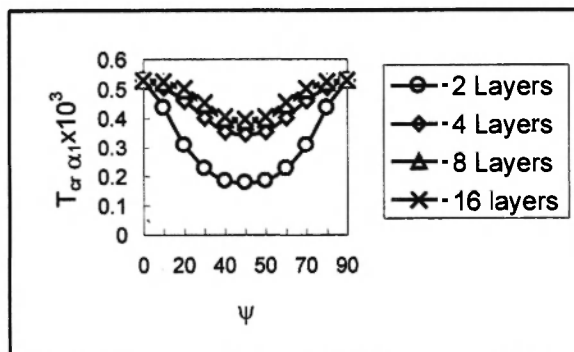
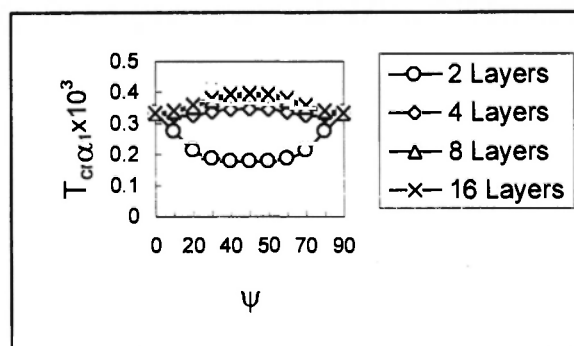


Fig. 1(b): Geometry of a typical two-layered laminated square plate

Clamped



Simply Supported

Fig. 2: Effect of ply orientation on the critical buckling temperature of laminates ( $a/t = 20$ ,  $a/b = 1$ )

However, the reverse phenomenon is observed in two-layer laminates. This is because bending-stretching coupling stiffness reach their maximum values at stacking layers  $N=2$  and decrease rapidly as  $N$  increases.

Figure 3 gives a summary of the buckling modes predictions for  $N = 2$ . We note that the eigenvalue of the first buckling mode or (eigenmode) is smaller than the eigenvalue of the second buckling mode, and so on. These buckling modes are the same for  $N = 4$ ,  $N = 8$  and  $N = 16$ .

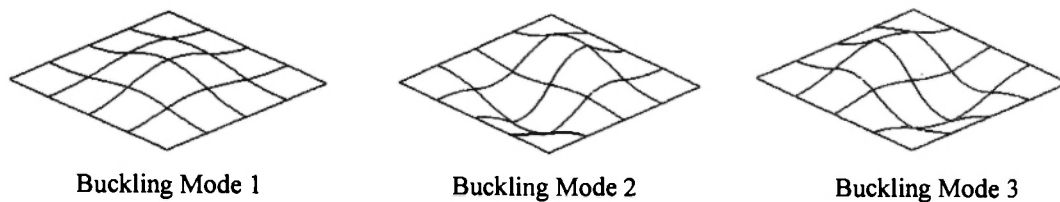


Fig. 3: Buckling modes of a laminated square plate

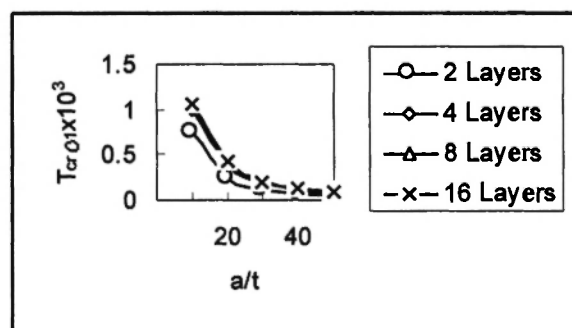
### Effect of plate thickness ratio

Figure 4 depicts the effects of plate thickness ratio  $a/t$  on the critical buckling temperature for a square laminated plates having lamination angle  $\psi = 45^\circ$ . It is shown that the thermal buckling loads decrease with an increase in laminate thickness. This is in agreement with Ref. /10/. It is evident that the rigidity and hence the critical temperature decreases rapidly as the plate thickness ratio increases. This is because the stiffness of the laminate is greatly reduces when it becomes relatively thin. The effect of the number of stacking layers  $N$  on  $T_{cr}$  is insignificant when  $a/t$  is large.

### Effect of aspect ratio $a/b$

The effect of aspect ratio  $a/b$  on the critical temperature is illustrated in Figure 5. It can be seen that  $T_{cr}$  goes up as the plate aspect ratio increases. Since geometry has a significant influence on in-plane loaded structures, it is expected that the buckling load of a laminate will be greatly influenced by the change in the plate geometry. However, for a thermally loaded laminate, the graph shows that at  $a/b \geq 1.2$  the critical buckling temperature increases proportionally with the increase in the aspect ratio. There is no change of the buckling mode shape with the variation of aspect ratio,

Clamped



Simply Supported

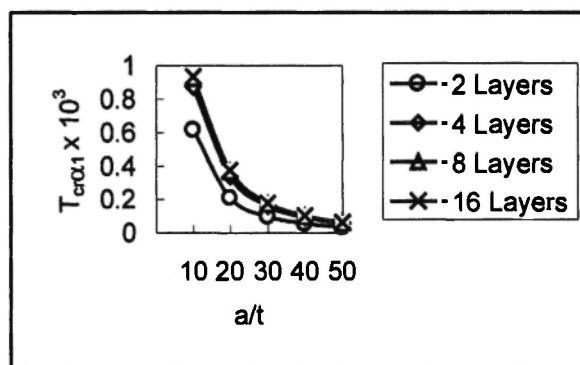
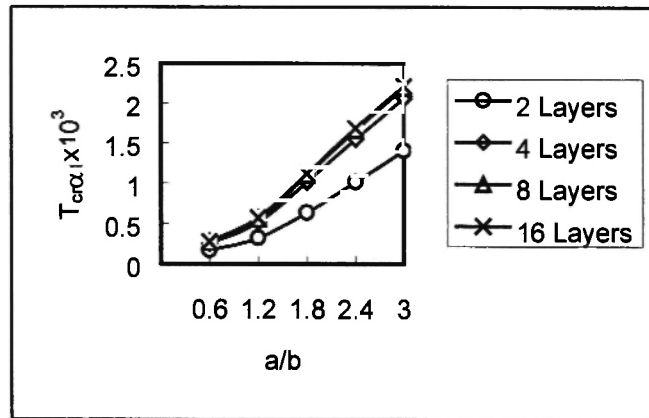
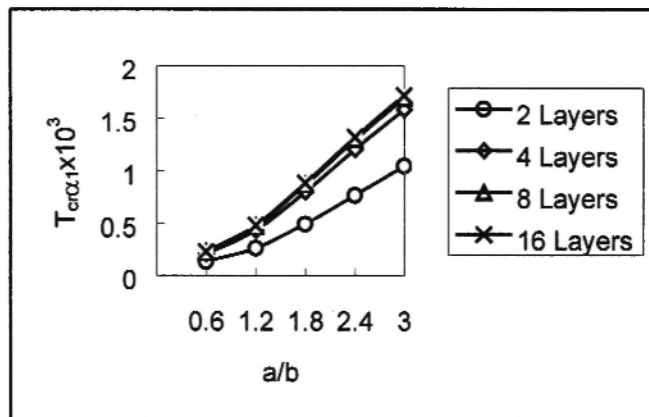


Fig. 4: Effect of plate thickness on the critical buckling temperature of laminates ( $a/b = 1$ ,  $\psi = 45^\circ$ )

**Clamped****Simply Supported****Fig. 5:** Effect of aspect ratio on the critical buckling temperature of laminates ( $a/t = 20$ ,  $\psi = 450$ )

since the curves go up smoothly without any cusp, more especially for  $a/b > 1.8$ .

The buckling mode shapes for different aspect ratios are shown in Figure 6 below.

### The effect of the modulus ratio $E_1 / E_2$

Figure 7 shows the influence of the modulus ratio  $E_1/E_2$  on critical buckling temperature. It is observed that in a simply supported plate of  $N = 4$ ,  $N = 8$  and  $N = 16$ ,  $T_{cr}$  increases with increase of modulus ratio and

plotted curves are rather flat when  $E_1/E_2 \geq 10$ . The increase in the number of layers means an increase in the material substance and hence the rigidity of a laminate. The interaction of the various stiffnesses means greater ability of the laminate to withstand buckling loads. For simply supported edges, Figure 7 shows that the boundaries have less influence on the modulus ratio of a laminate. The graph of  $N = 2$  for the simply supported and clamped plates shows that the plate is more susceptible to buckling as a result of the change in  $E_1/E_2$ .



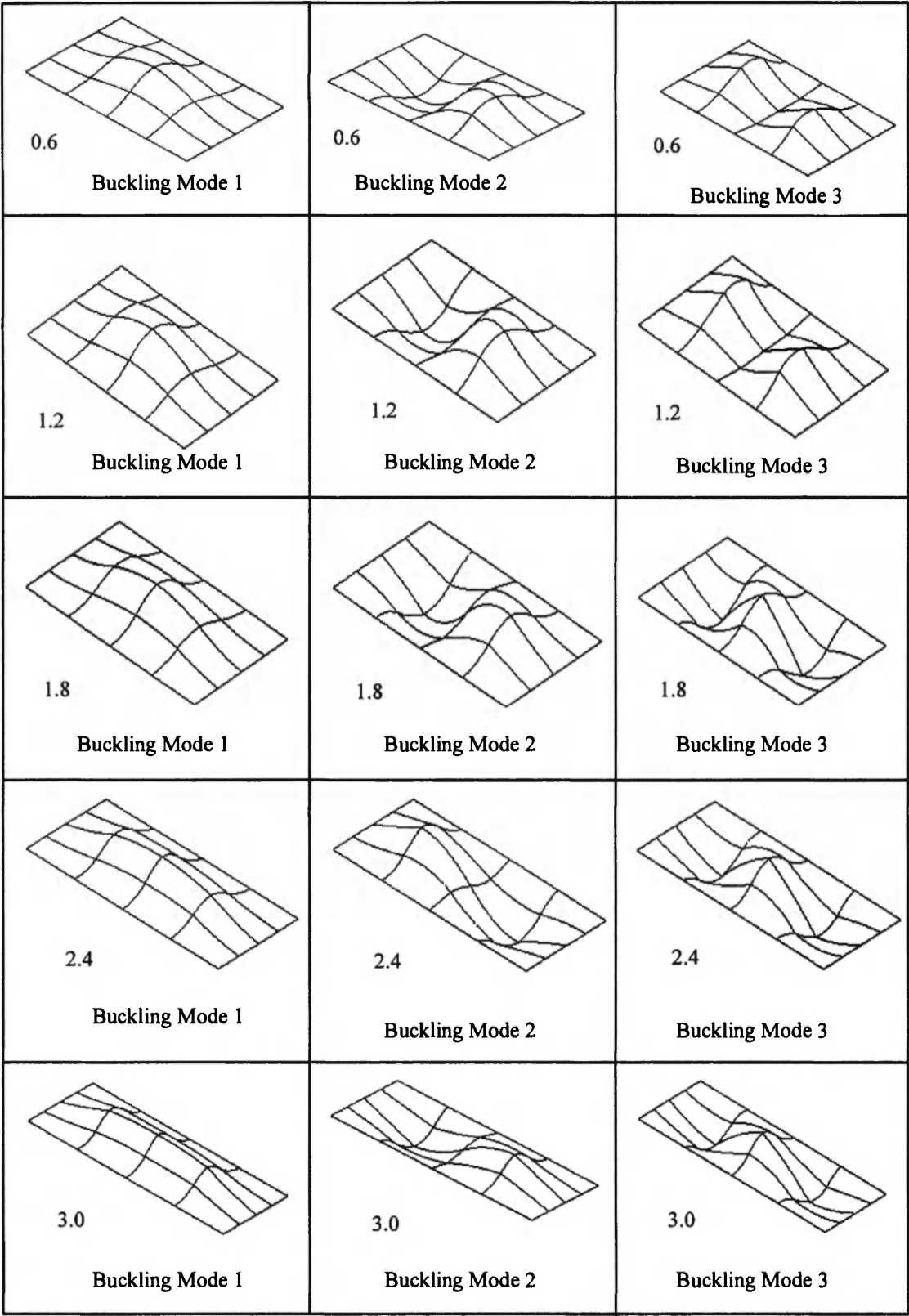


Fig. 6: Buckling mode shapes for each of the aspect ratios

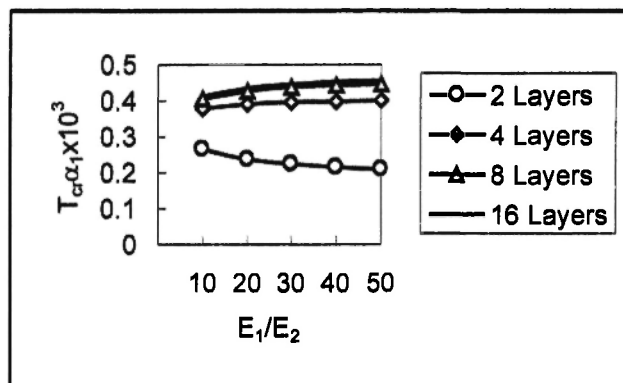
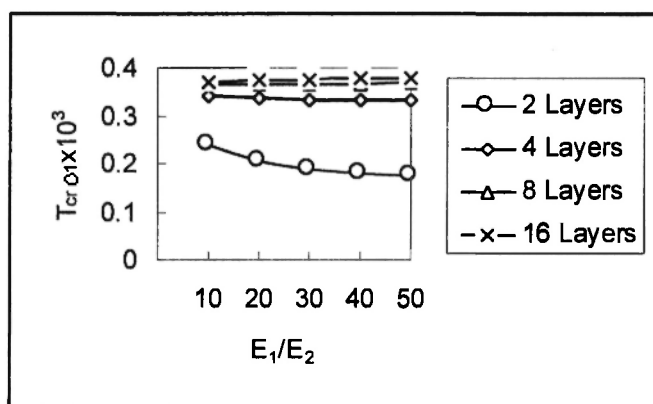
**Clamped****Simply Supported**

Fig. 7: Effect of the modulus ratio on the critical buckling temperature of laminates ( $a/b = 1$ ,  $a/t = 20$ ,  $\psi = 450$ )

### The effect of thermal expansion coefficient ratio $\alpha_2/\alpha_1$

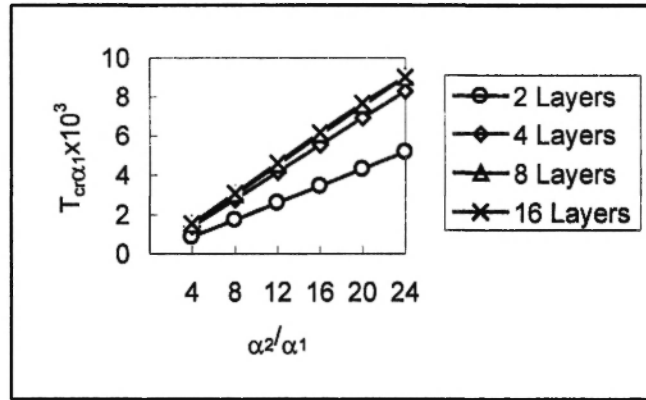
The effect of thermal expansion coefficient ratio  $\alpha_2/\alpha_1$  on the critical temperature is shown in Figure 8. The higher the ratio of thermal expansion coefficients, the higher the value of  $T_{cr}$ . This means that the thermal coefficient of expansion has a linear relationship with the buckling temperature of a laminate. It is pointed out that in the present analysis  $\alpha_1$  was varied while  $\alpha_2$  was left constant. An increase in the coefficient of expansion means that more temperature has to be applied to cause buckling on a laminated composite. The interaction of the different coefficients of the different materials in a laminate has a tendency to increase the temperature needed to cause buckling. We note that in Ref. /4/ the

opposite trend is observed for  $T_{cr}$  versus  $\alpha_2/\alpha_1$  as  $\alpha_1$  is varied. The expansion coefficients of a laminated composite have a direct influence on the buckling temperature as expected from the strain equation (5).

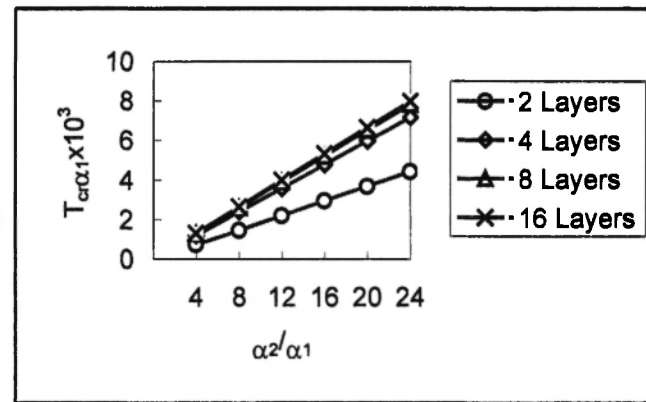
### The effect of boundary conditions

Figure 9 shows the effect of boundary condition on the variation of critical temperature. The boundary condition has a strong impact on the critical temperature  $T_{cr}$ , as shown in the figure. Also, the variation of  $T_{cr}$  for different aspect ratios is presented in Figure 9 for both simply supported and clamped plates with  $N = 4$  in order to compare the effect of the boundary condition. It can be seen that the critical temperatures of clamped

Clamped



Simply Supported



**Fig. 8:** Effect of thermal expansion ratio on the critical buckling temperature of laminates ( $a/b = 1$ ,  $a/t = 20$ ,  $\psi = 450$ )

cases are higher than those of the simply supported cases. This is because of the enhanced stiffness of the laminate by the clamping of the laminate. The simply

supported edges make the plate susceptible to buckling, as the edges are not restricted from expanding. The effect of the aspect ratio was presented in Figure 5.

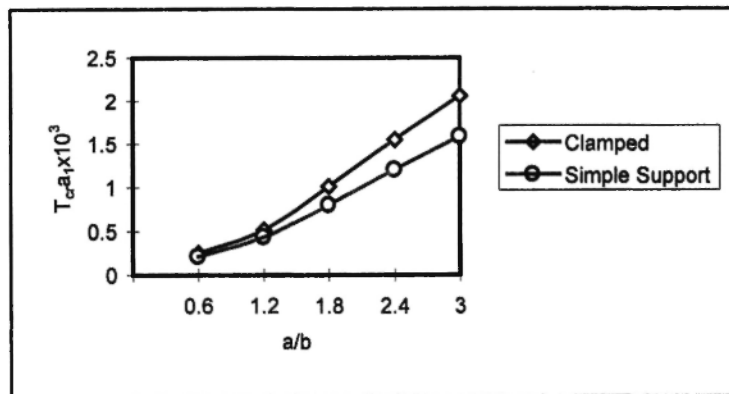


**Fig. 9:** Influence of boundary condition and aspect ratio on the critical buckling temperature of laminates ( $a/t = 20$ ,  $N = 4$ ,  $\psi = 450$ )

## CONCLUSION

The performance of laminated composites under adverse temperature variation dictates that careful analysis be made to determine the optimum configuration of the composite structures. It has been seen that of all the variables that were used to study the behaviour of a laminated plate, the number of layers affects the buckling temperature the most. For two layers, the bending-stretching coupling is at the maximum and as the number of layers increases, the laminate approaches orthotropy and the critical buckling temperature decreases. The effects of lamination angle, aspect ratio, and material parameter, etc have a significant influence on the critical buckling temperature of laminated plates.

## ACKNOWLEDGEMENT

The authors would like to thank the Foundation for Research Development (now referred to as the NRF, the National Research Fund) for its financial assistance. The technical support of Peninsula Technikon and the support from the Centre for Research in Applied Technology is acknowledged.

## REFERENCES

1. C. Shaikh, V.E. Verijenko, P.Y. Tabakov and S. Adali, Higher-Order Theory of Laminated Composites under Thermal and Static Loading, *Proc. of the 2nd South African Conference on Applied Mechanics*. Vol. 2, pp. 913-924, 1998.
2. M. Zeggane and S. Sridharan, Stability analysis of long laminated composite plates using Reissner-Mindlin 'infinite' strips, *Computers and Structures*, **40** (4), 1033-1042 (1991).
3. K. Chandrashekhara, Thermal buckling of laminated plates using a shear flexibility finite element, *Finite Elements in Analysis and Design*, **12**, 51-61 (1992).
4. W.J. Chen, P.D. Lin and L.W. Chen, Thermal buckling behaviour of thick composite laminated plates under non-uniform temperature distribution, *Computers and Structures*, **41** (4), 637-645 (1991).
5. T.C. Mathew, G. Singh and G.V. Rao, Thermal buckling of cross-ply composite laminates, *Computers and Structures*, **42** (2), 281-287 (1992).
6. R.D. Mindlin, Influence of rotatory inertia and shear on flexural motions of isotropic, elastic plates, *J. Appl. Mech.* 31-38 (1954).
7. E. Reissner, The effect of transverse shear deformation on the bending of elastic plates, *J. Appl. Mech.* Vol. 12 (1945).
8. K. Bath, *Finite Element Procedures*, Prentice-Hall, Englewood, New Jersey, 1996.
9. R.M. Jones, *Mechanics of Composite Materials*, McGraw-Hill, Kogakusha, Tokyo, 1975.
10. P. Simelane and B. Sun, Thermal buckling analysis of laminated composite plates, *Proceedings of the 2nd SA Conference of Applied Mechanics'98*, Vol.2, 925-936, Cape Town, 1998.
11. R.M. Wung and J.N. Reddy, A transverse deformation theory of laminated composite plates, *Computers and Structures*, **41** (4), 821-833 (1991).
12. B.H. Sun, The buckling theory based on the generalised variational principle, *Report of the ASME Winter Annual Meeting*, 1993.
13. ABAQUS/Standard User's Manual, Vol. 1 and Vol. 2, Version 5.6.
14. ABAQUS/Example Problems Manual, Vol. 1 and Vol. 2, Version 5.6.
15. ABAQUS Theory Manual